

# High Efficiency Dual-Integrated Stacked Microstructured Solid-State Neutron Detectors

S.L. Bellinger, *Member, IEEE*, R.G. Fronk, W.J. McNeil, T.J. Sobering, D.S. McGregor, *Member, IEEE*

**Abstract— Silicon diodes with large aspect ratio perforated microstructures backfilled with  ${}^6\text{LiF}$  show a dramatic increase in neutron detection efficiency beyond that of conventional thin-film coated planar devices. Described in this work are advancements in the technology using detector stacking methods to increase thermal neutron detection efficiency. The highest efficiency devices thus far have delivered over 42% intrinsic thermal neutron detection efficiency by device-coupling stacking methods. The detectors operate as conformally diffused  $pn$  junction diodes each having  $1\text{cm}^2$  square-area. Two individual devices were mounted back-to-back with counting electronics coupling the detectors together into a single dual-detector device. The solid-state silicon device operated at 3V and utilized simple signal amplification and counting electronic components. The intrinsic detection efficiency for normal-incident 0.0253 eV neutrons was found by calibrating against a calibrated  ${}^3\text{He}$  proportional counter.**

## I. INTRODUCTION

Microstructured semiconductor neutron detectors have been developed and studied at Kansas State University for many years [1-5], with much improvement in recent times [6-8]. The microstructured detector design offers a viable solution to the efficiency limitations of coated planar diodes, a limitation no greater than 5% [9]. The microstructured detector concept is understood as a method to improve detection efficiency [10-12], with the first such device demonstrated nearly a decade ago [1]. In recent times, many other groups are now investigating microstructured semiconductor detectors [13-15].

The devices are constructed by etching microstructured features into a semiconductor substrate, diffusing a  $pn$  junction within the microstructures, and subsequently backfilling the etched features with neutron reactive material. The individual device structure has the potential of achieving intrinsic thermal neutron detection efficiencies,  $\epsilon_m$ , greater than 35% [8]. In addition, with proper alignment, two microstructured devices may be combined to compose a single detector with double the efficiency as a single microstructured device.

In the present work, the backfilled neutron reactive material is  ${}^6\text{LiF}$ , which relies on the  ${}^6\text{Li}(n,t){}^4\text{He}$  reaction. When thermal neutrons are absorbed by  ${}^6\text{Li}$ , a 2.73 MeV triton and a 2.05 MeV alpha particle are ejected in opposite directions. These reaction products are much more energetic than those of the  ${}^{10}\text{B}(n,\alpha){}^7\text{Li}$  or  ${}^{157}\text{Gd}(n,\gamma){}^{158}\text{Gd}$  reactions, such that the measured signal to noise ratio is larger, thereby improving discrimination of background radiations.  ${}^6\text{Li}$  has a relatively large microscopic thermal neutron absorption cross section of 940 b. In addition, the stable compound  ${}^6\text{LiF}$  was used instead of the highly reactive lithium metal.

The present work employs previous technological methods [16], in conjunction with stacking dual-integrated detectors to achieve unmatched solid state neutron detection efficiency. With recent advancements in inductively-coupled-plasma reactive-ion-etching (ICP-RIE) using high-aspect ratio deep etching (HARDE) techniques, along with common MEMS wet-etching techniques [6,16-18], unique neutron detector microstructures have been realized. Wet-etched strait trench microstructured diode devices have been fabricated and backfilled with  ${}^6\text{LiF}$  neutron absorber material. Simulated expected multi-channel analyzer measured spectra for different microstructured patterns and neutron reactive backfilled materials has been previously investigated to provide predictive information for optimal device design configurations, see [2,8,19-20]<sup>1</sup>.

The focus of this work involved mounting two detector chips back-to-back, along with counting electronics, and coupling them together into a single detector device. Previous work has been completed with this device [6-7]; hereon, an effort has been made to improve the detection efficiency of the device by modifying the charge-sensing detection circuitry to account for longer charge integration time. For the improved dual detector device, the intrinsic detection efficiency for normal incident 0.0253 eV neutrons was found by calibrating the detector against a calibrated  ${}^3\text{He}$  proportional counter [21]. An important clear advantage for the 3D microstructured neutron detectors is the high efficiency achieved with a single device, which can be doubled with stacked configurations.

## II. NEUTRON DETECTOR FABRICATION

Initially, an oxide was grown on a 10 k $\Omega$ -cm  $n$ -type Si wafer in which a diffusion window was patterned and the oxide was partially removed. Silicon microstructures were

---

Manuscript received November 13, 2010. This work is supported in part by the Defense Threat Reduction Agency, contract DTRA-01-03-C-0051, National Science Foundation, Grant DE-FG07-04ID14599, and the US Department of Energy, NEER Program grant No. DE-FG07-04ID14599.

S.L. Bellinger, (telephone: 785-532-7087, e-mail: slb3888@ksu.edu), R.G. Fronk, W.J. McNeil, D.S. McGregor are with the SMART Laboratory of Kansas State Univ., Manhattan, KS USA 66506. T.J. Sobering is with the Electronics Design Laboratory of Kansas State Univ., Manhattan, KS USA 66506

---

<sup>1</sup> Note that in refs. [8,19-20] the reaction product particle energies were inadvertently switched for the  ${}^{10}\text{B}(n,\alpha){}^7\text{Li}$  neutron reaction. These switched energies are typographical errors and were not included in the Monte Carlo simulations. The calculated pulse-height spectra produced in refs. [8,19-20] are correct.

then etched into the Si diffusion windows with a 45% KOH wet-etch submersion process at 70°C; the trench pattern, masked in the residual oxide of the diffusion window, was aligned to the <111> planes in a (110) orientated Si wafer. Individual detectors were batch processed on 3 inch diameter wafers, each with an active square-area of 1cm<sup>2</sup>. The devices reported in the present work have strait trenches etched 250 microns deep by 25 microns wide, where the trenches are periodically spaced 50 microns apart. The strait trench design maintains high neutron detection efficiency while creating an opportunity to off-set stack the detector chips so as to maximize neutron absorption; for further detail see [6-7].

After the etch process, the wafer was chemically cleaned and *p*-type regions were diffused uniformly into individual device microstructures across the wafer, thereby forming *pn* junctions within the trenches. A Ti-Au metal contact was evaporated on the backside of the wafer to make an electrical ground contact, thereby completing the diode structure and enabling depletion through the bulk of the individual devices. Finally, <sup>6</sup>LiF powder was packed into the trenches to function as the neutron absorbing converter material (see Figs. 1 and 2). The LiF material was synthesized by reacting LiOH and HF to precipitate solid LiF in 1 - 20 micron cubic granules [22]. The coarse LiF powder was then reduced to nanopowder through a vapor transport condensation method. The LiF nanopowder packs densely into the trenches with little to no void fraction.

Individual device chips were then mounted as dual-integrated detector systems. The dual detector amplifying and readout electronics were specifically designed in-house and consists of a sandwiched detector board and a separate motherboard (see Fig. 3), see also [7]. The separate motherboard configuration was used for research purposes as it simplifies testing multiple detector types through the use of common electronics [7]. In this configuration, the contacts of each detector are common and applied to the input of a charge sensitive preamp. In earlier work, a relatively short charge integration time of 2 μs was used [7]; it was found in [7] that the charge drifts slowly in the weak electric potential field of the microstructure diode, a consequence of the conformal diffusion design. Charge drift simulations were completed in [7] and predicted a full charge integration time, for a 250 micron deep trench microstructured diode, of 10 μs. Therefore, the preamp was reconfigured for a longer charge integration time of 10 μs.

### III. NEUTRON DETECTION MEASUREMENTS

Neutron counting efficiency was measured with a 0.0253 eV diffracted neutron beam from the Kansas State University TRIGA Mark II nuclear reactor [23]. The neutron flux was calibrated with a Reuter-Stokes <sup>3</sup>He gas-filled proportional detector and found to be  $1.05 \pm 0.02 \times 10^3 \text{ n cm}^{-2} \text{ s}^{-1}$ . Details of the calibration method can be found elsewhere [21].

A pulse-height spectrum was collected from the stacked dual-integrated microstructured detector in the diffracted neutron beam with and without a beam blocking Cd shutter so as to allow the collection of responses with and without thermal-neutrons. Prompt gamma-rays emitted from the thin

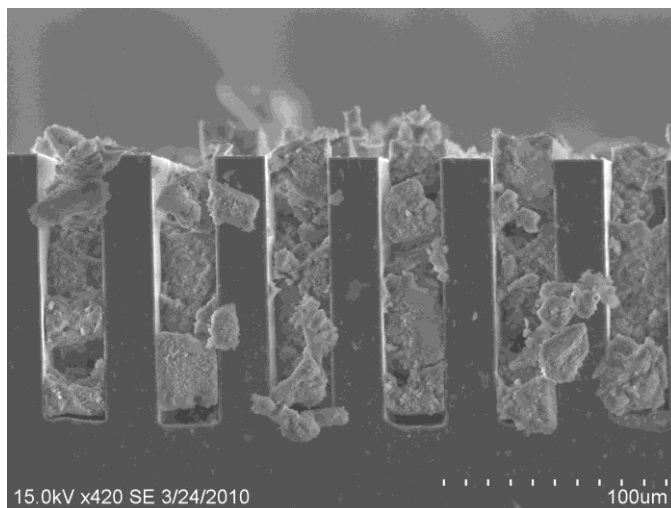


Fig. 1. <sup>6</sup>LiF nanopowder backfilled into the wet-etched strait trench microstructures 100 microns deep.

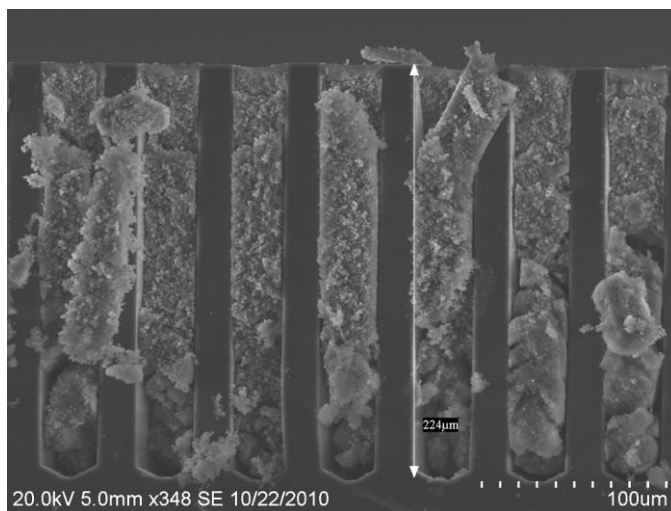
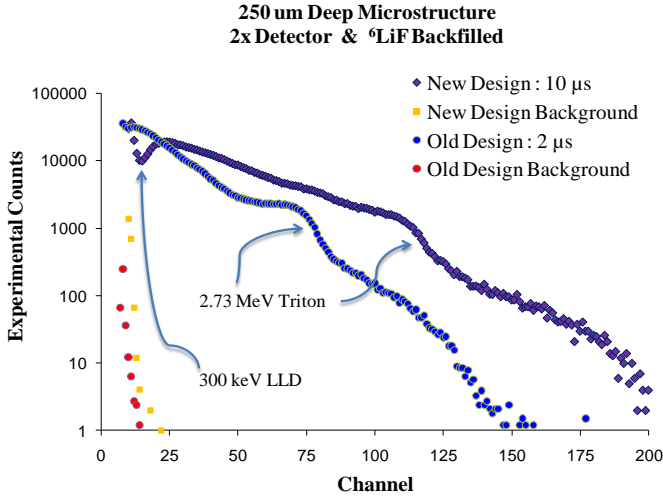


Fig. 2. <sup>6</sup>LiF nanopowder backfilled into the wet-etched strait trench microstructures 224 microns deep.



Fig. 3. Shown are dual-integrated packaged devices with preamplifying circuitry. The motherboard, which provides an adjustable detector bias, bias current compensation, pulse shaping and gain, an analog output for pulse-height analysis, and a “digital” output from a discriminator, is show elsewhere [7].



**Fig. 4.** Pulse-height spectra comparison of the previous 2  $\mu\text{s}$  charge integration-time preamp old design versus the improved 10  $\mu\text{s}$  charge integration-time preamp new design for the dual-integrated 250  $\mu\text{m}$  deep straight trench microstructure backfilled with  ${}^6\text{LiF}$ . At an LLD = 15 Chn (300 keV), the measured thermal neutron detection  $\epsilon_{\text{th}}$  was 42% for the 10  $\mu\text{s}$  charge integration-time preamp design.

Cd shutter appear in the spectrum as numerous pulses at low energy near the noise floor of the detector system (see Fig. 4). The neutron counting efficiency was calculated by dividing the summed neutron counts, collected from the dual detector with a LLD (lower level discriminator) set above the system noise, by the calibrated flux determined with the  ${}^3\text{He}$  detector.

Fig. 4 shows the measured pulse-height spectrum from the dual-integrated device, with each detector chip having 250 micron deep trenches. The single dual-integrated device works well with as little as 2 volts of applied bias. The total leakage current for the  $1\text{cm}^2$  dual-integrated devices was 500 nA [7]. Note that in Fig. 4, the old preamp design pulse-height spectrum is shifted to lower channels than shown elsewhere for shallower trench depth designs [21,24]. Some of this shift may have been due to an overall increase in capacitance of the stacked device, thereby reducing the pulse height signal from the detector. Another component of this downward shift was discovered elsewhere [7], where from semiconductor modeling simulations it was determined that, due to the conformal diffusion microstructured diode design, the signal integration time is on the order of 10  $\mu\text{s}$ . By increasing the preamp charge integration time to 10  $\mu\text{s}$  for the same device, the thermal neutron irradiation pulse-height spectrum (see Fig. 4) has shifted higher, away from the noise/gamma-ray floor of the neutron counting system and exhibits the expected spectral shape predicted elsewhere [8].

Similar to the other tested devices with the Cd shutter closed [25], the gamma-ray component was negligible at an LLD setting above channel 11 for the 2  $\mu\text{s}$  signal integration time design and channel 15 for the 10  $\mu\text{s}$  signal integration time design. As previously reported, with the LLD set to channel 11 (375 keV), the intrinsic efficiency for the 2  $\mu\text{s}$  signal integration time design was measured to be  $37.0 \pm 0.6\%$ . For the 10  $\mu\text{s}$  signal integration time design, with the LLD set to channel 15 (300 keV), the intrinsic efficiency was measured to be  $42.0 \pm 0.25\%$ .

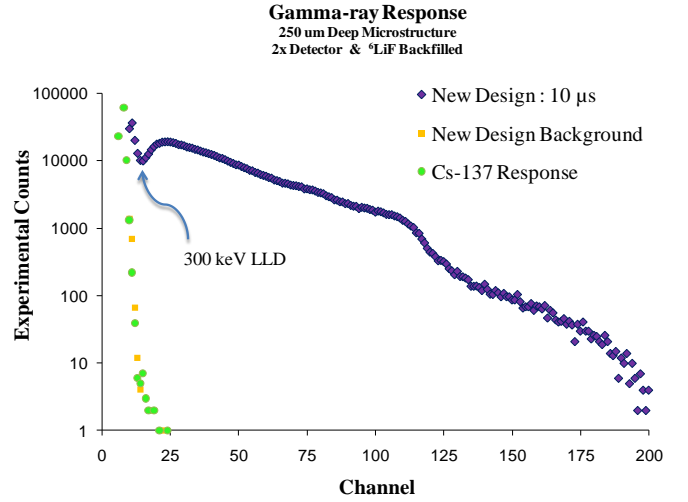


**Fig. 5.** Measured  ${}^{137}\text{Cs}$  gamma-ray irradiation and neutron irradiation pulse-height spectral features for the dual-integrated neutron detector with the 10  $\mu\text{s}$  signal integration time design.

The actual gamma-ray flux with the Cd shutter in place was not measured; however, the gamma-ray response for the detector was determined using a  ${}^{137}\text{Cs}$  source placed 10 cm from the device, with a source activity of 0.72 mCi for an irradiation time of 10 minutes. The gamma-ray pulse-height spectrum response is shown in Fig. 5. Notice that the response of the dual-integrated detector is relatively equivalent to that of the Cd shutter detector response.

In addition, notice the spectral shape of the 10  $\mu\text{s}$  signal integration time design spectra in Fig. 4 corresponds well with the expected results calculated elsewhere, in which a dip in the spectrum appears in the lower energy region of the pulse-height spectrum [8]. This fortuitous dip in the pulse height spectrum at low energies allows for the trench design to be operated with an increased LLD setting over other microstructured designs [8], thereby improving gamma-ray discrimination, without severely reducing the detector efficiency. Deeper microstructured trenches and dual-integrated devices show a slight reduction in pulse height, which can decrease the  $n/\gamma$  ratio. Yet, in the present work, this pulse height shift does not appear to be severe, and has sufficiently moved away from the noise floor with the increase preamp charge integration time. Note that the gamma-ray interactions within the device also diminish with deeper perforations (due to less interaction volume), thereby allowing for smaller LLD settings resulting in superior gamma-ray discrimination.

#### IV. CONCLUSIONS

A dual-integrated,  $1\text{cm}^2$  straight trench microstructured Si detector, backfilled with  ${}^6\text{LiF}$  powder has been characterized for neutron sensitivity in a diffracted 0.0253 eV thermal neutron beam from a TRIGA Mark II nuclear reactor. An important clear advantage for the dual-integrated microstructured neutron detector design is the high efficiency achieved by appropriately stacking two detector chips into a single device. Efficiency is dramatically increased by

capturing streaming neutrons from the first detector. The dual-integrated detector with two 250 micron deep trenched devices achieved 42% intrinsic efficiency, which is a total increase of 5% efficiency over the previous preamplifying circuitry design. Finally, the gamma-ray rejection for the dual-integrated stacked device was high, with prompt Cd and  $^{137}\text{Cs}$  gamma rays in the low energy to noise end of the pulse height spectrum, which is due to many combined effects explained elsewhere [8].

To improve charge capture efficiency and shorten the signal integration time, future work will be dedicated to fabrication of interlaced microstructures that are etched from both sides of the Si diode, shown elsewhere [26]; therefore, the electric field will be uniformly distributed across the Si detector volume and the signal integration time necessary to collect all the produced charge will be reduced and not limited by increased microstructure depth.

#### REFERENCES

- [1] D.S. McGregor et al., "New Surface Morphology for Low Stress Thin-Film-Coated Thermal Neutron Detectors," *IEEE Trans. Nuclear Science*, NS-49, pp. 1999-2004, 2002.
- [2] J.K. Shultis and D.S. McGregor, "Efficiencies of Coated and Perforated Semiconductor Neutron Detectors," *IEEE Trans. on Nuclear Science*, NS-53, pp. 1659-1665, 2006.
- [3] W.J. McNeil et al., "Development of Perforated Si Diodes for Neutron Detection," *IEEE Nuclear Science Symposium*, Oct. 29-Nov. 3 2006.
- [4] Q. Jahan, E. Patterson, B. Rice, W.L. Dunn, and D.S. McGregor, "Neutron Dosimeters Employing High-efficiency Perforated Semiconductor Detectors," *Nuc. Instrum. and Meth.*, vol. B263, pp. 183-185, 2007.
- [5] C.J. Solomon, J.K. Shultis, W.J. McNeil, B.B. Rice, and D.S. McGregor, "A Hybrid Method for Coupled Neutron-Ion Transport Calculations for 10B and 6LiF Coated and Perforated Detector Efficiencies," *Nuclear Instruments and Methods*, vol. A580, pp. 326-330, 2007.
- [6] S.L. Bellinger et al., "Characteristics of the Stacked Microstructured Solid-State Neutron Detector," *SPIE proc.*, 2010, in Press.
- [7] S.L. Bellinger, R.G. Fronk, W.J. McNeil, T.J. Sobering, and D.S. McGregor, "Enhanced variant designs and characteristics of the microstructured solid-state neutron detector," *Nucl. Instr. and Meth.*, 2010, in Press.
- [8] J.K. Shultis and D.S. McGregor, "Design and Performance Considerations for Perforated Semiconductor Thermal-Neutron Detectors," *Nuclear Instruments and Methods*, vol. A606, pp. 608-636, 2009.
- [9] D.S. McGregor, M.D. Hammig, H.K. Gersch, Y-H. Yang, and R.T. Klann, "Design Considerations for Thin Film Coated Semiconductor Thermal Neutron Detectors, Part I: Basics Regarding Alpha Particle Emitting Neutron Reactive Films," *Nuclear Instruments and Methods*, vol. A500, pp. 272-308, 2003.
- [10] R.A. Muminov and L.D. Tsvang, "High-Efficiency Semiconductor Thermal-Neutron Detectors," *Soviet Atomic Energy*, vol. 62, no. 4, pp. 316-319, 1987.
- [11] J. Schelten, M. Balzhauser, F. Hongesberg, R. Engels, and R. Reinartz, "A New Neutron Detector Development Based on Silicon Semiconductor and  $^6\text{LiF}$  Converter," *Physica B*, vol. 234-236, pp. 1084-1086, 1997.
- [12] C.P. Allier, *Micromachined Si-well scintillator pixel detectors*. Netherlands: DUP Science, 2001.
- [13] J. Uher et al., "Characterization of 3D thermal neutron semiconductor detectors," *Nuclear Instruments and Methods*, vol. A576, pp. 32-37, 2007.
- [14] A.M. Conway, T.F. Wang, N. Deo, C.L. Cheung, and R.J. Nikolic, "Numerical Simulations of Pillar Structured Solid State Thermal Neutron Detector: Efficiency and Gamma Discrimination," *IEEE TNS*, vol. 56, no. 5, pp. 2802-2807, October 2009.
- [15] J. Dingley, Y. Danon, N. LiCausi, J.Q. Lu, and I. B. Bhat, "Optimization of a Novel Solid-State Self Powered Neutron Detector," in *Int. Conf. on Math., Comp. Meth. & Reactor Physics*, LaGrange Park, 2009.
- [16] S.L. Bellinger, W.J. McNeil, and D.S. McGregor, "Improved Fabrication Technique for Microstructured Solid-State Neutron Detectors," *Proc. MRS*, vol. 1164, 2009.
- [17] S.L. Bellinger, W.J. McNeil, T.C. Unruh, and D.S. McGregor, "Characteristics of 3D Micro-Structured Semiconductor High Efficiency Neutron Detectors," *IEEE Transactions on Nuclear Science*, vol. 56, no. 3, June 2009.
- [18] K.E. Bean and R.J. Lawson, "Application of Silicon Crystal Orientation and Anisotropic Effects to the Control of Charge Spreading in Devices," *IEEE Journal of Solid-State Circuits*, vol. SC-9, no. 3, pp. 111-117, June 1974.
- [19] J.K. Shultis and D.S. McGregor, "Calculation of Ion Energy-Deposition Spectra in Silicon, Lithium-Fluoride, Boron, and Boron Carbide," Kansas State University, Engineering Experiment Station 299, April 2004.
- [20] D.S. McGregor et al., "Perforated Diode Neutron Detector Modules Fabricated from High-Purity-Silicon," *Radiation Physics and Chemistry*, no. 78, pp. 195-207, 2009.
- [21] D.S. McGregor, W.J. McNeil, S.L. Bellinger, T.C. Unruh, and J.K. Shultis, "Microstructured Semiconductor Neutron Detectors," *Nuclear Instruments and Methods*, vol. A608, pp. 125-131, 2009.
- [22] D.S. McGregor et al., "Perforated Semiconductor Neutron Detector Modules," *Proc. of 32nd Annual GOMACTech Conf.*, March 2007.
- [23] T.C. Unruh, "Development of a neutron diffraction system and neutron imaging system for beamport characterization," Kansas State University, Thesis 2009.

- [24] D.S. McGregor, S.L. Bellinger, W.J. McNeil, and T.C. Unruh, "Micro-Structured High-Efficiency Semiconductor Neutron Detectors," *2008 IEEE Nuclear Science Symposium Conference Record*, R15-2, pp. 446-448, 2008.
- [25] S.L. Bellinger, W.J. McNeil, and D.S. McGregor, "Variant Designs and Characteristics of Improved Microstructured Solid-State Neutron Detectors," *IEEE Nuclear Science Symposium Conference Record*, N14-4, pp. 986-989, 2009.
- [26] D.S. McGregor and R.T. Klann, "High-Efficiency Neutron Detectors and Methods of Making the Same," US-7,164,138, January 16, 2007.